

Supporting information

Coexistence of Spin Canting and Metamagnetism in a One-Dimensional Mn(II) Compound Bridged by Alternating Double End-to-End and Double End-On Azido Ligands and the Analog Co(II) Compound. ‡

Nesrine Benamara ^a, Zouaoui Setifi ^{a,b}, Chen-I Yang ^{c,*}, Sylvain Bernès ^d, David K. Geiger ^e, Güneş Süheyla Kürkçüoğlu ^f, Fatima Setifi ^{a,*} and Jan Reedijk ^{g,*}

^a Laboratoire de Chimie, Ingénierie Moléculaire et Nanostructures (LCIMN), Université Ferhat Abbas Sétif 1, Sétif 19000, Algeria

^b Département de Technologie, Faculté de Technologie, Université 20 Août 1955-Skikda, Skikda 21000, Algeria

^c Department of Chemistry, Tunghai University, Taichung 407, Taiwan

^d Instituto de Física, Benemérita Universidad Autónoma de Puebla, 72570 Puebla, Pue., Mexico

^eDepartment of Chemistry, SUNY-College at Geneseo, Geneseo, NY 14454, USA

^fDepartment of Physics, Eskişehir Osmangazi University, 26040 Eskişehir, Turkey

^gLeiden Institute of Chemistry, Leiden University, P.O. Box 9502, 2300 RA Leiden, The Netherlands.

Table of contents

Figure S1. Experimental (black) and simulated (red) XRD powder patterns for complexes **1** (top) and **2** (bottom). Simulated patterns were generated using Mercury software (CCDC, see ref. 9 in main manuscript) with $\lambda = 1.54 \text{ \AA}$ and the single-crystal structure refinements. In the pattern of **1**, the low-angle peak marked with an asterisk is probably due to the sample holder. A calculated baseline was subtracted in both experimental patterns.

Figure S2. FT-IR data of compounds **1-2**.

Figure S3. Plot of X_{M-1} (circles) vs. temperature for a powdered sample of compound **1**.

The solid line represents the best fit X_{M-1} above 110 K with a Curie-Weiss law.

Figure S4. Plot of $X_M T$ vs. T of powdered samples of compound **1** in an applied field of 100 Oe from 2 to 300 K.

Figure S5. ZFC/FC magnetizations of compound **1** at the field of 10 Oe.

Figure S6. X' and X'' plots of ac magnetic susceptibilities in a zero applied dc field and in an ac field of 3.5 G at the indicated frequencies for a powdered sample of compound **1**.

Figure S7. The blow-up of the hysteresis loop of compound **1** at 1.8 K.

Figure S8: FC magnetization curves measured under different external fields for compound **1**.

Figure S9. Field dependence of magnetizations for compound **1** measured at the indicated temperatures.

Figure S10. dM/dH vs. H plots for the virgin magnetization of compound **1**

Figure S11. Plot of X_M (circles) vs. temperature for a powdered sample of compound **2**.

Figure S12. Plot of X_{M-1} (circles) vs. temperature for a powdered sample of compound **2**. The solid line represents the best fit X_{M-1} above 100 K with a Curie-Weiss law.

Figure S13. X' and X'' plots of ac magnetic susceptibilities in a zero applied dc field and in an ac field of 3.5 Oe at the indicated frequencies for a powdered sample of compound **2**.

Figure S14. Field dependence of the magnetization of compound **2** (Co) at 2.0 K. The inset gives a blow-up of the hysteresis loop.

Figure S15. Plots of the temperature dependence of M' and M'' of the ac magnetic susceptibilities of thermally decomposed compound **1** in a zero applied dc field and in an ac field of 3.5 Oe at the indicated frequencies.

Figure S16. Field dependence of the magnetization of thermally decomposed compound **1** at 1.8 K. The insets give the low field range of M vs. H .

Figure S17. Field-dependent magnetization of the thermally decomposed compound **2** at 2.0 K. The inset gives a low field range of M vs H .

Figure S18. Plots of the temperature dependence of M' and M'' of ac magnetic susceptibilities of thermal decomposed compound **2** in a zero applied dc field and in an ac field of 3.5 G at the indicated frequencies.

Table S1. Recompilation of magneto-structural data for azido-bridged compounds reported in the literature.

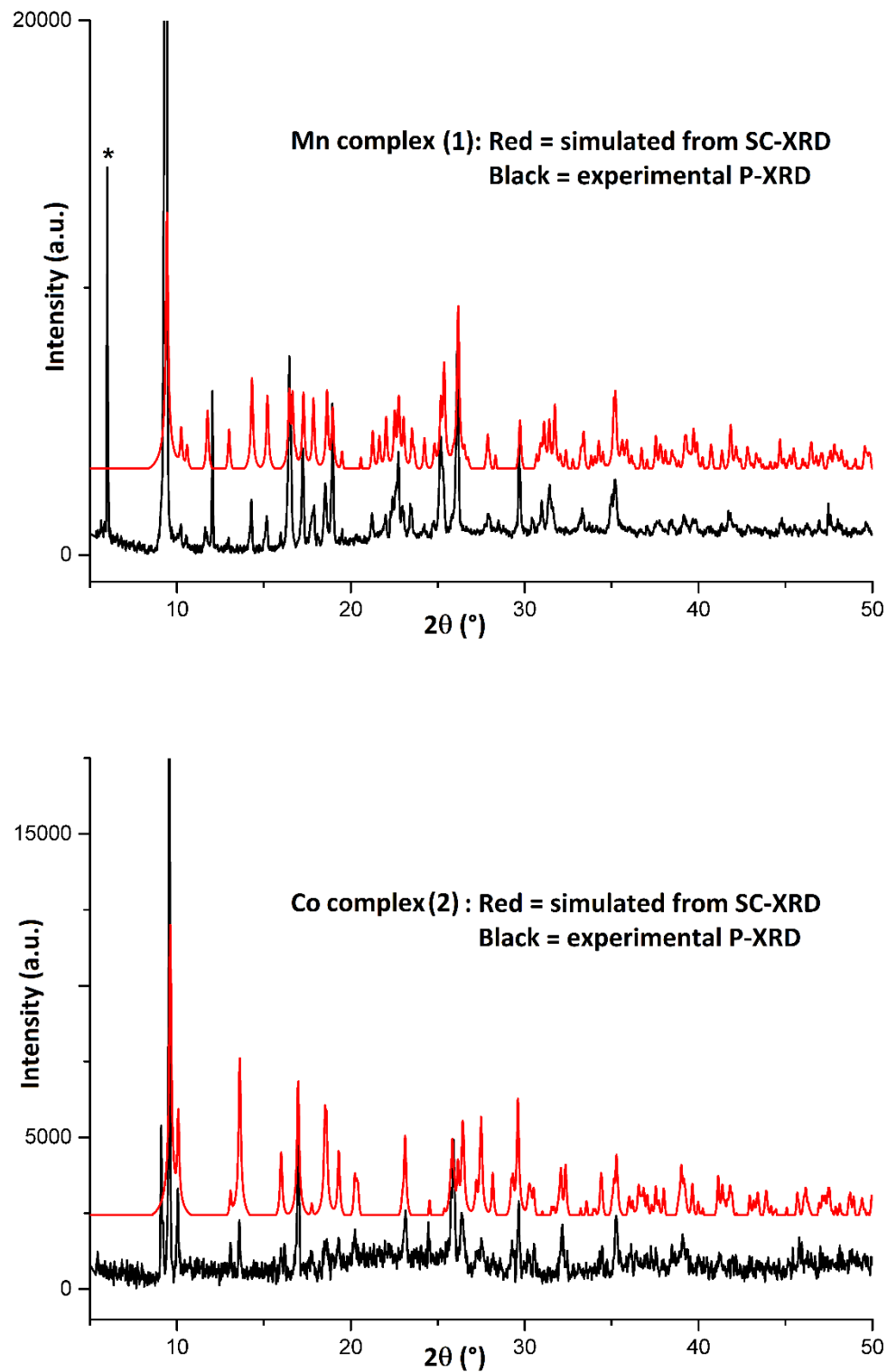


Figure S1. Experimental (black) and simulated (red) XRD powder patterns for complexes **1** (top) and **2** (bottom). Simulated patterns were generated using Mercury software (CCDC, see ref. 9 in main manuscript) with $\lambda = 1.54 \text{ \AA}$ and the single-crystal structure refinements. In the pattern of **1**, the low-angle peak marked with an asterisk is probably due to the sample holder. A calculated baseline was subtracted in both experimental patterns.

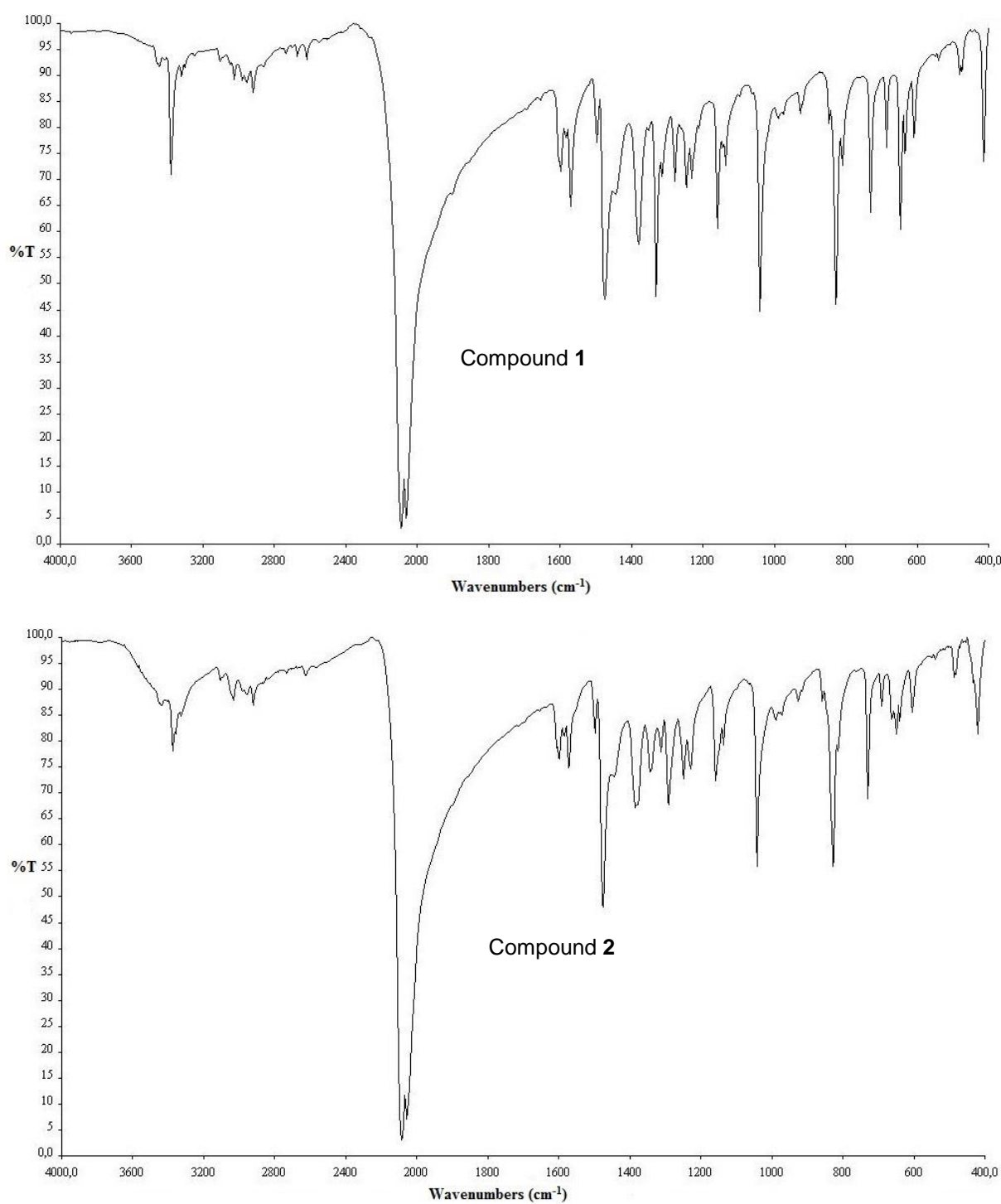


Figure S2. FT-IR data of compounds **1** (Mn) and **2** (Co).

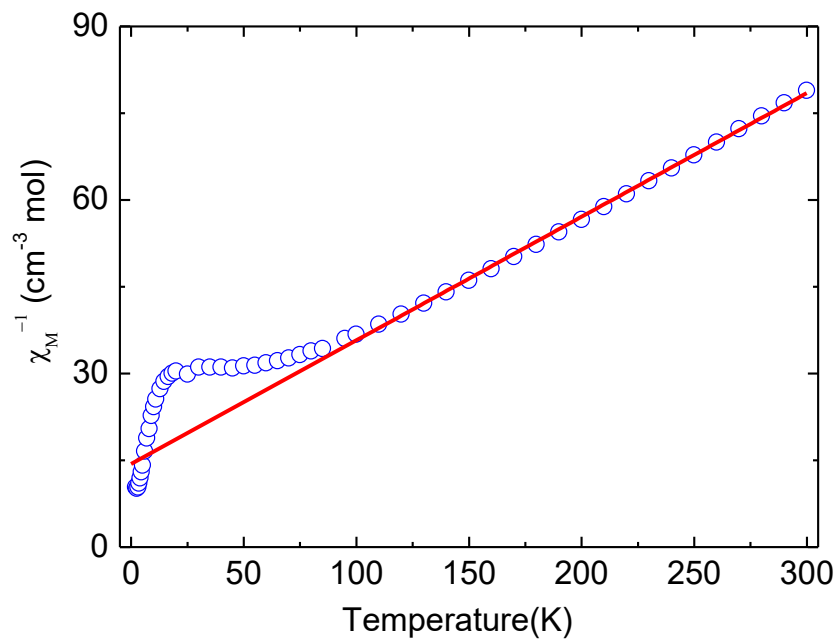


Figure S3. Plot of χ_M^{-1} (circles) vs. temperature for a powdered sample of compound **1**. The solid line represents the best fit χ_M^{-1} above 110 K with a Curie-Weiss law.

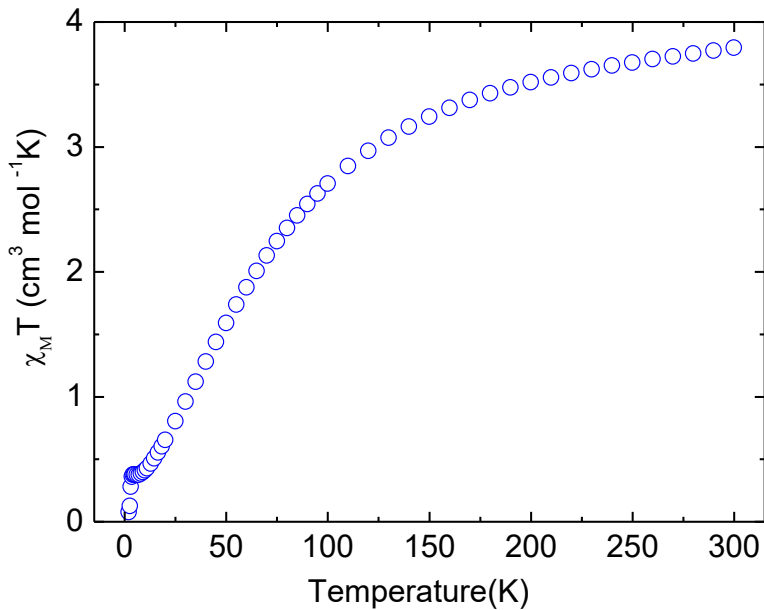


Figure S4. Plot of $\chi_M T$ vs. T of powdered samples of compound **1** in an applied field of 100 Oe from 2 to 300 K.

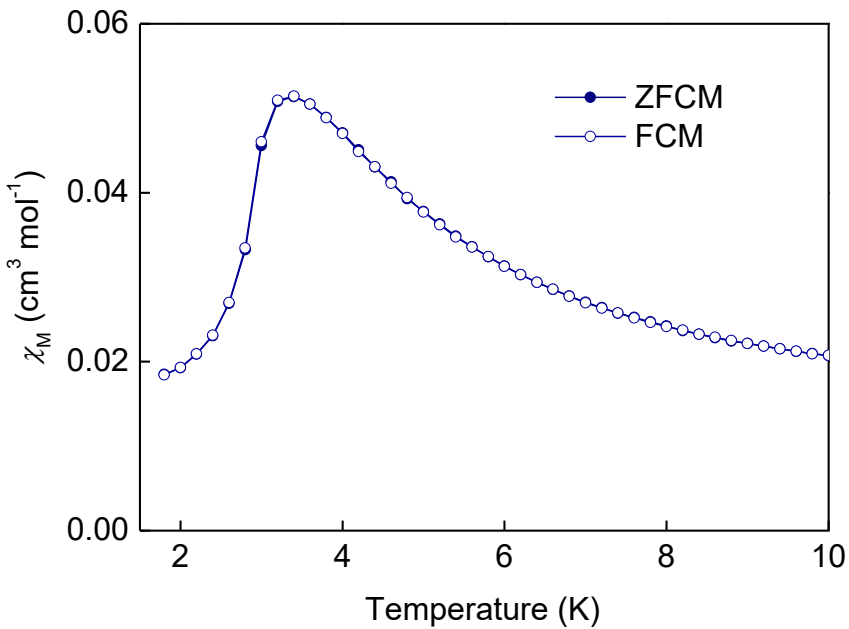


Figure S5. ZFC/FC magnetizations of compound **1** at the field of 10 Oe.

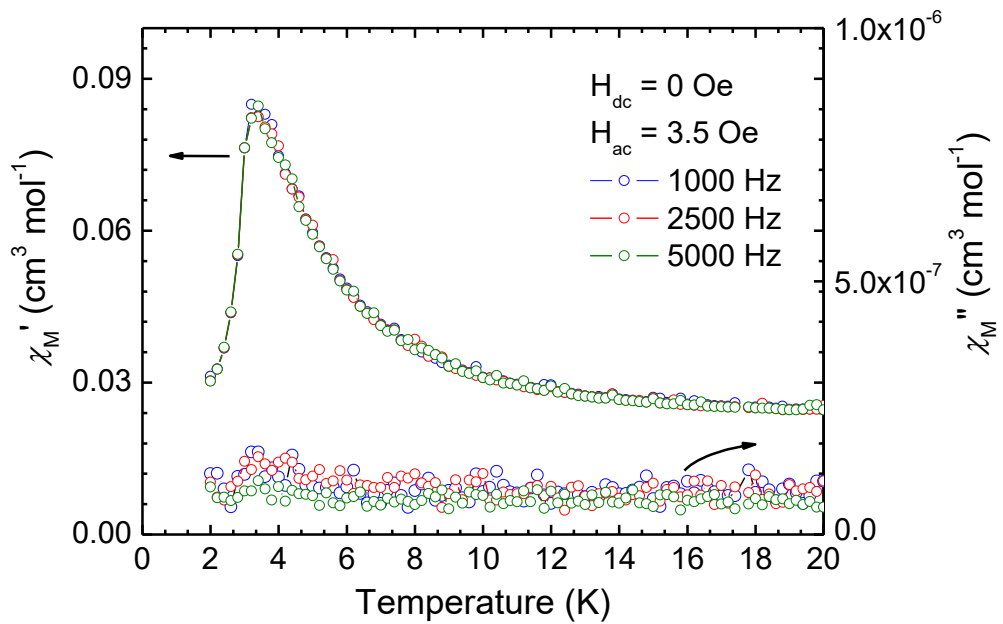


Figure S6. χ' and χ'' plots of ac magnetic susceptibilities in a zero applied dc field and in an ac field of 3.5 G at the indicated frequencies for a powdered sample of compound **1**.

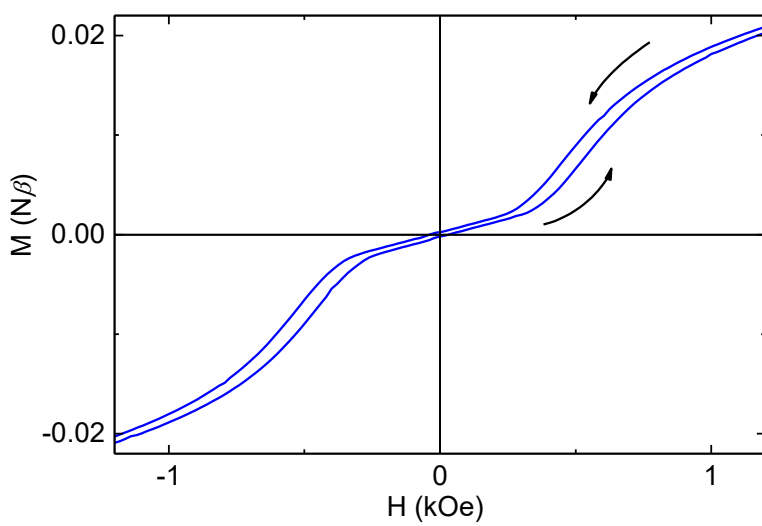


Figure S7. The blow-up of the hysteresis loop of compound **1** at 1.8 K.

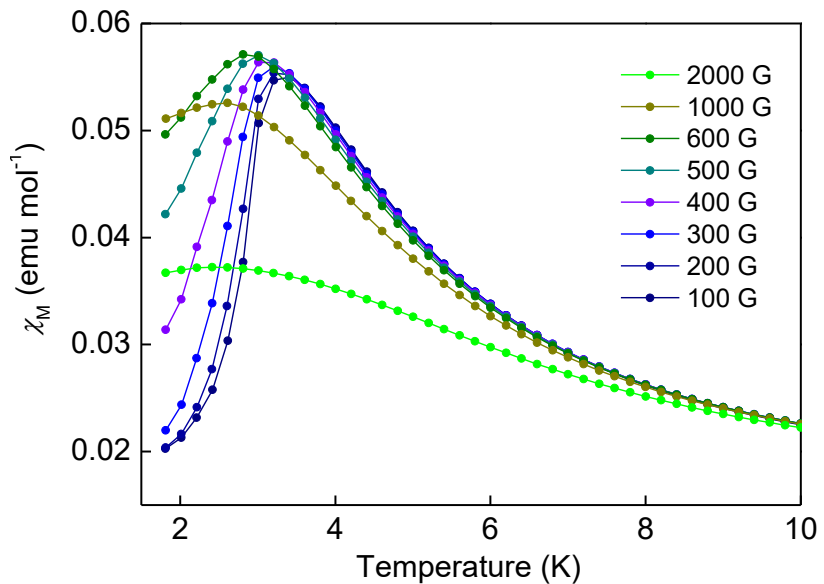


Figure S8. FC magnetization curves measured under different external fields for compound **1**.

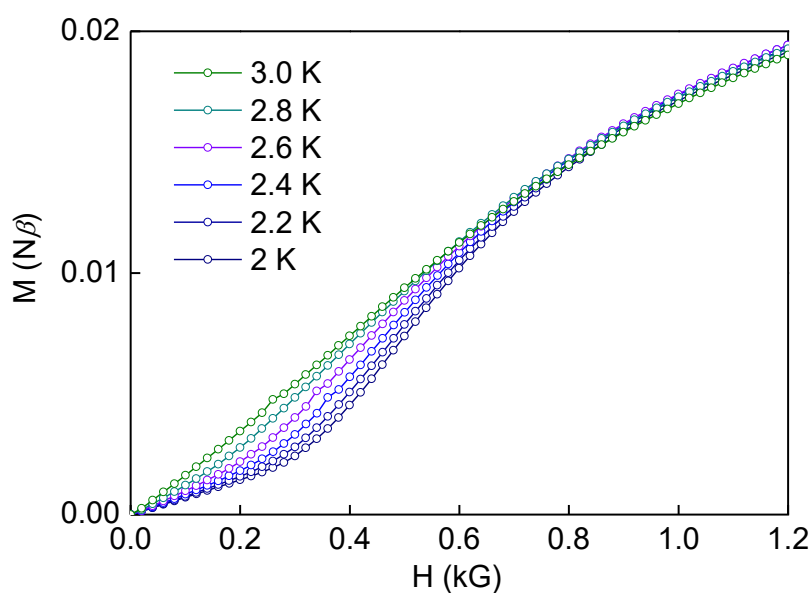


Figure S9. Field dependence of magnetizations for compound 1 measured at the indicated temperatures.

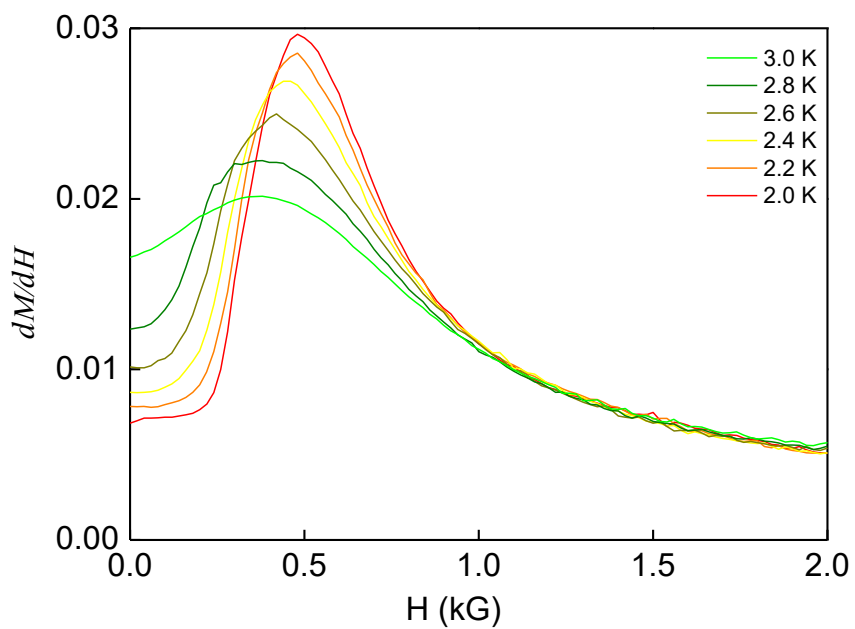


Figure S10. dM/dH vs. H plots for the virgin magnetization of compound 1...

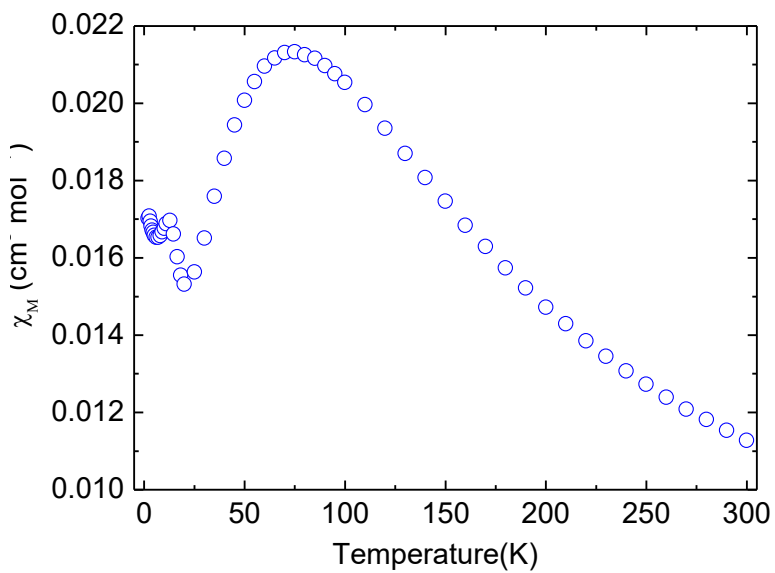


Figure S11. Plot of χ_M (circles) vs. temperature for a powdered sample of compound **2**.

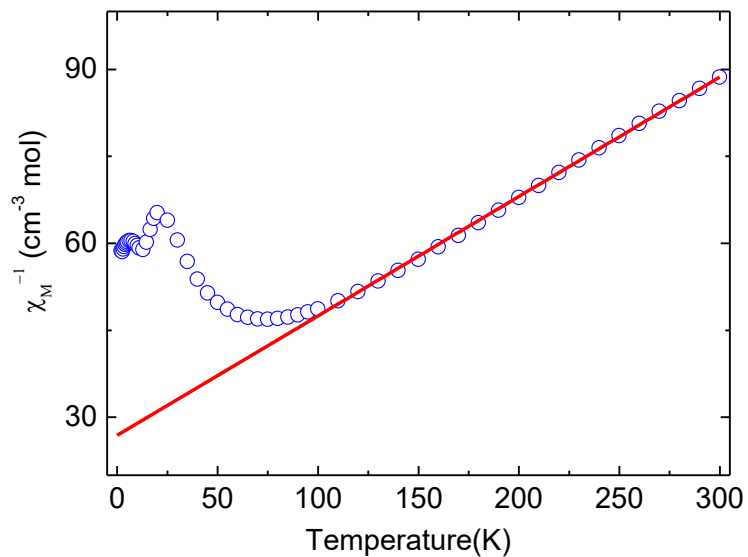


Figure S12. Plot of χ_M^{-1} (circles) vs. temperature for a powdered sample of compound **2**. The solid line represents the best fit χ_M^{-1} above 100 K with a Curie-Weiss law.

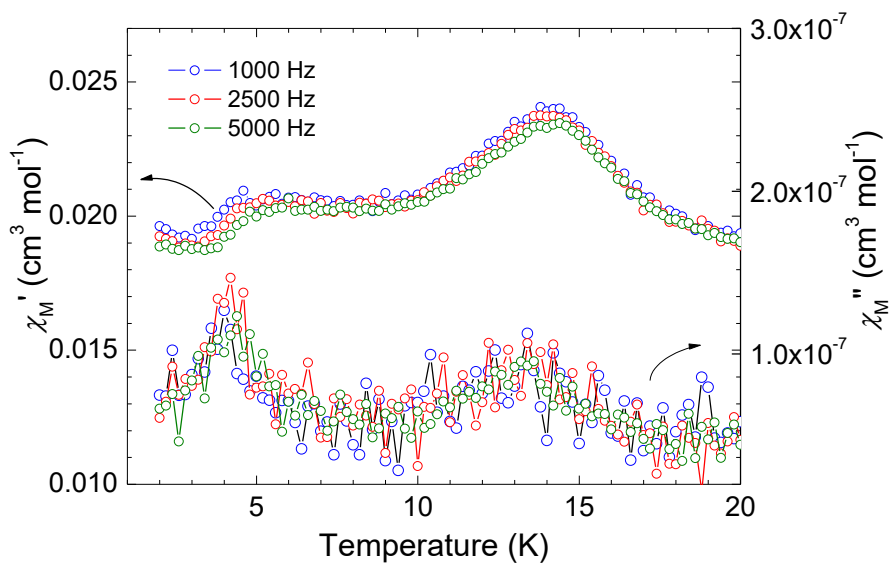


Figure S13. χ' and χ'' plots of ac magnetic susceptibilities in a zero applied dc field and in an ac field of 3.5 Oe at the indicated frequencies for a powdered sample of compound **2**.

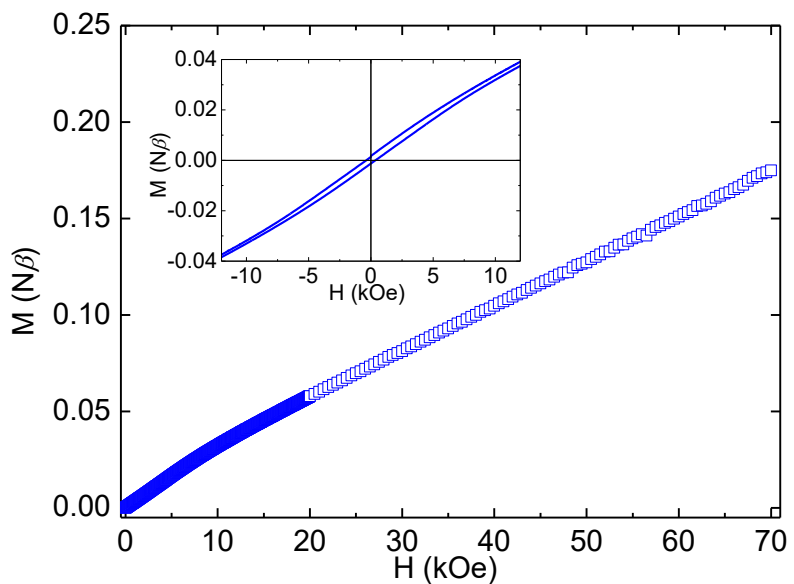


Figure S14. Field dependence of the magnetization of compound **2** (Co) at 2.0 K. The inset gives a blow-up of the hysteresis loop.

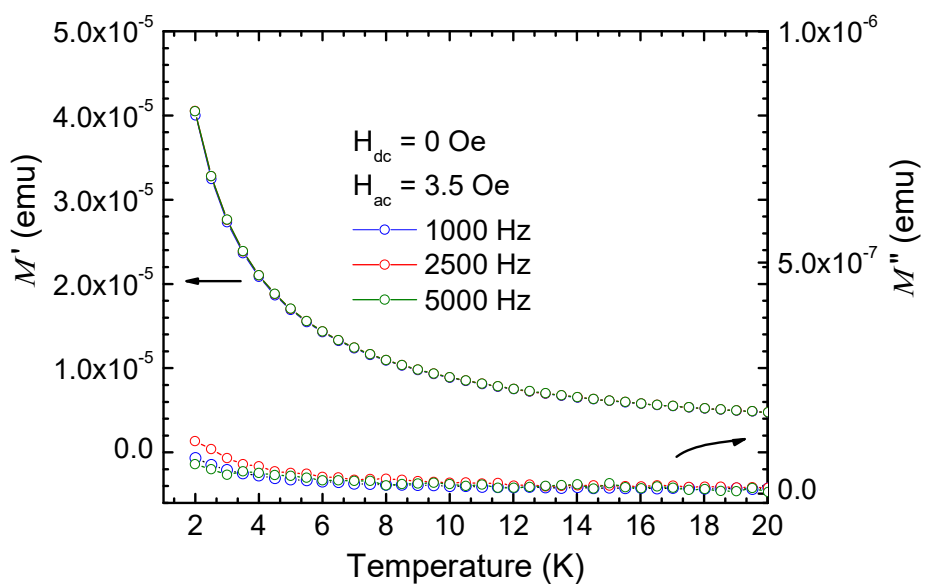


Figure S15. Plots of the temperature dependence of M' and M'' of the ac magnetic susceptibilities of thermally decomposed compound **1** in a zero applied dc field and in an ac field of 3.5 Oe at the indicated frequencies.

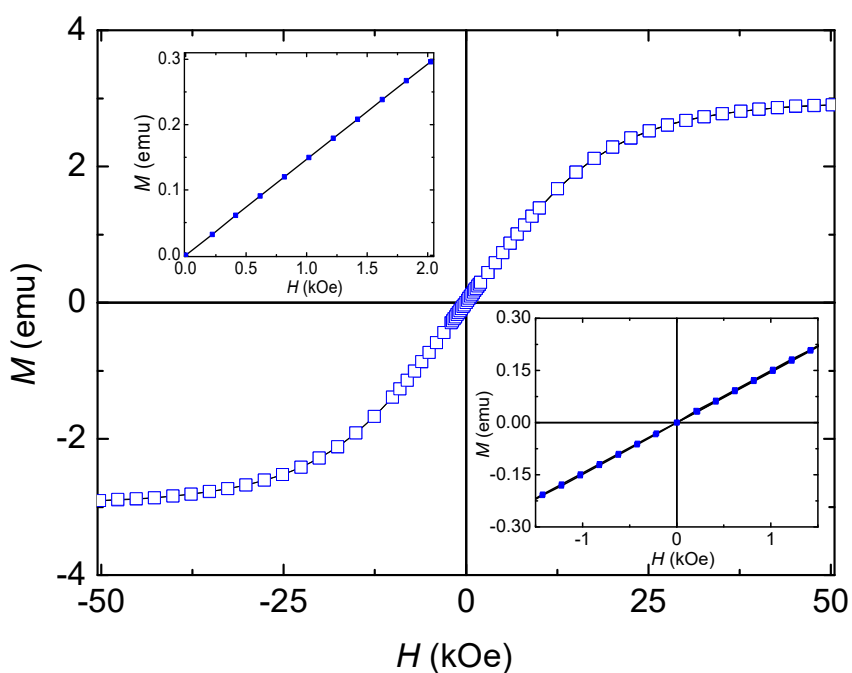


Figure S16. Field dependence of the magnetization of thermally decomposed compound **1** at 1.8 K. The insets give the low field range of M vs. H .

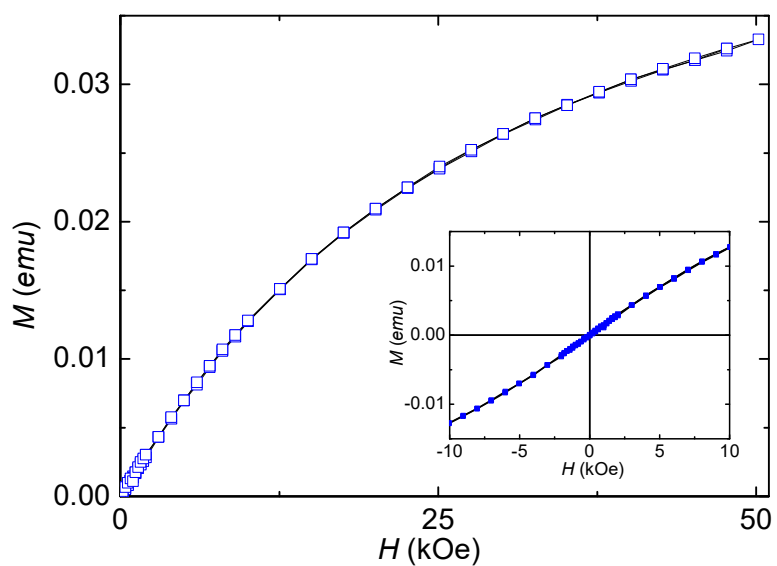


Figure S17. Field-dependent magnetization of the thermally decomposed compound **2** at 2.0 K. The inset gives a low field range of M vs H .

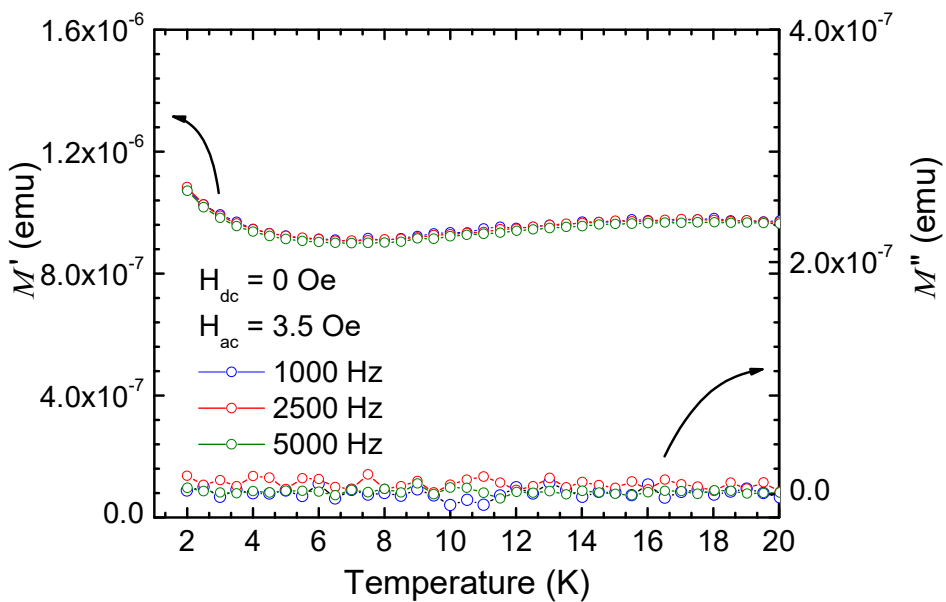


Figure S18. Plots of the temperature dependence of M' and M'' of ac magnetic susceptibilities of thermal decomposed compound **2** in a zero applied dc field and in an ac field of 3.5 G at the indicated frequencies.

Table S1. Recompilation of magneto-structural data for azido-bridged compounds reported in the literature. Only 1D polymeric systems alternating EO and EE double azido bridges along the chain for which crystal structures and magnetic coupling constants are available have been retained. The $M\ldots M$ distances and δ dihedral angles were obtained using *Mercury* and the CSD deposited CIF files.

CSD Refcode	Metal	$M\ldots M$ for EO bridge (Å)	$M\ldots M$ for EE bridge (Å)	δ angle for EE bridge (°)	J_F / J_{AF} (cm ⁻¹)	reference
DOHDEK	Mn(II)	3.443	5.416	26.95	7.8 / -10.8	a
DOLDIS	Mn(II)	3.431	5.409	19.76, 20.28	7.7 / -11.2	a
GOQKIG	Mn(II)	3.402	5.149	31.69	2.4 / -13.7	b
CUQDEX	Mn(II)	3.416	5.229	26.56	3.5 / -12.3	c
IBIGOP	Mn(II)	3.480	5.432	35.09	45.3 / -53.3	d
IQASOI	Mn(II)	3.461	5.404	19.61	5.6 / -11.9	e
IRIHIA	Mn(II)	3.481	5.400	1.82	2.7 / -14.5	f
MIJKIA	Mn(II)	3.407	5.418	11.85	0.2 / -10.4	g
QEKGIW	Mn(II)	3.496	5.484	20.48	15.7 / -67.6	h
UJACAJ	Mn(II)	3.406	5.394	9.80	3.8 / -15.4	i
UJACEN	Mn(II)	3.444, 3.435	5.465	7.96, 10.52	5.2 / -11.8	i
UJACIR	Mn(II)	3.517	5.311	19.46	7.2 / -13.7	i
UJACOX	Mn(II)	3.413	5.484	9.80	4.1 / -13.3	i
UJACUD	Mn(II)	3.509	5.332	11.95	8.0 / -14.4	i
VECDIR	Mn(II)	3.440	5.466	7.62	1.6 / -13.9	j
XANFAU	Mn(II)	3.408	5.287	9.77	6.0 / -16.7	k
YEVHAI	Mn(II)	3.454	5.343	22.70	9.6 / -11.8	l, m, o
-	Mn(II)	3.422	5.430	9.69	2.87 / -11.3	This work
-	Co(II)	3.361	5.317	25.20	n.d. / n.d.	This work
QOWSIF	Co(II)	3.406	5.365	18.03	n.d. / n.d.	n
NAYHUQ	Ni(II)	3.249	5.117	35.21	26.0 / -2.6	o
ZIJFUT	Ni(II)	3.224	5.180	2.72	77.0 / -187.1	p, q
ZIJGAA	Ni(II)	3.218, 3.240	5.112	17.97, 25.35	73.0 / -28.5	p, q
HOTDEZ	Cu(II)	3.486	5.383	11.34	7.6 / -60.5	r

a) Yan-Feng Yue, En-Qing Gao, Chen-Jie Fang, Tao Zheng, Jue Liang, Chun-Hua Yan, *Cryst.Growth Des.* (2008), 8, 3295, doi:[10.1021/cg800138x](https://doi.org/10.1021/cg800138x)

b) M.A.M. Abu-Youssef, A. Escuer, M.A.S. Goher, F.A. Mautner, R. Vicente, *Eur.J.Inorg.Chem.* (1999), 687, doi: [10.1002/\(SICI\)1099-0682\(199904\)1999:4<687::AID-EJIC687>3.0.CO;2-E](https://doi.org/10.1002/(SICI)1099-0682(199904)1999:4<687::AID-EJIC687>3.0.CO;2-E)

- c) M.A.M.Abu-Youssef, A.Escuer, D.Gatteschi, M.A.S.Goher, F.A.Mautner, R.Vicente, *Inorg.Chem.* (1999), **38**, 5716, doi:[10.1021/ic990656x](https://doi.org/10.1021/ic990656x)
- d) M.Villanueva, J.L.Mesa, M.K.Urtiaga, R.Cortes, L.Lezama, M.I.Arriortua, T.Rojo, *Eur.J.Inorg.Chem.* (2001), 1581, doi:[10.1002/1099-0682\(200106\)2001:63.3.CO;2-U](https://doi.org/10.1002/1099-0682(200106)2001:63.3.CO;2-U)
- e) En-Qing Gao, Shi-Qiang Bai, Chuan-Feng Wang, Yan-Feng Yue, Chun-Hua Yan, *Inorg.Chem.* (2003), **42**, 8456, doi:[10.1021/ic034618w](https://doi.org/10.1021/ic034618w)
- f) U.Ray, Sk.Jasimuddin, B.K.Ghosh, M.Monfort, J.Ribas, G.Mostafa, Tian-Huey Lu, C.Sinha, *Eur.J.Inorg.Chem.* (2004), 250, doi:[10.1002/ejic.200300415](https://doi.org/10.1002/ejic.200300415)
- g) Jian-Ying Zhang, Cai-Ming Liu, De-Qing Zhang, Song Gao, Dao-Ben Zhu, *Inorg.Chem.Commun.* (2007), **10**, 897, doi:[10.1016/j.inoche.2007.04.004](https://doi.org/10.1016/j.inoche.2007.04.004)
- h) Liang-Fu Tang, Lei Zhang, Li-Chun Li, Peng Cheng, Zhi-Hong Wang, Ji-Tao Wang, *Inorg.Chem.* (1999), **38**, 6326, doi:[10.1021/ic990878v](https://doi.org/10.1021/ic990878v)
- i) En-Qing Gao, Shi-Qiang Bai, Yan-Feng Yue, Zhe-Ming Wang, Chun-Hua Yan, *Inorg.Chem.* (2003), **42**, 3642, doi:[10.1021/ic0262987](https://doi.org/10.1021/ic0262987)
- j) Shi-Qiang Bai, En-Qing Gao, Zheng He, Chen-Jie Fang, Yan-Feng Yue, Chun-Hua Yan, *Eur.J.Inorg.Chem.* (2006), 407, doi:[10.1002/ejic.200500691](https://doi.org/10.1002/ejic.200500691)
- k) M.A.M.Abu-Youssef, A.Escuer, R.Vicente, F.A.Mautner, L.Ohrstrom, M.A.S.Goher, *Polyhedron* (2005), **24**, 557, doi:[10.1016/j.poly.2005.01.003](https://doi.org/10.1016/j.poly.2005.01.003)
- l) R.Cortes, L.Lezama, J.L.Pizarro, M.I.Arriortua, X.Solans, T.Rojo, *Angew.Chem.,Int.Ed.* (1995), **33**, 2488, doi:[10.1002/anie.199424881](https://doi.org/10.1002/anie.199424881)
- m) R.Cortes, M.Drillon, X.Solans, L.Lezama, T.Rojo, *Inorg.Chem.* (1997), **36**, 677, doi:[10.1021/ic961017e](https://doi.org/10.1021/ic961017e)
- n) Xiu-Teng Wang, Xiao-Hua Wang, Zhe-Ming Wang, Song Gao, *Inorg.Chem.* (2009), **48**, 1301, doi:[10.1021/ic801505a](https://doi.org/10.1021/ic801505a)
- o) G.Viau, M.G.Lombardi, G.De Munno, M.Julve, F.Lloret, J.Faus, A.Caneschi, J.M.Clemente-Juan, *Chem.Commun.* (1997), 1195, doi:[10.1039/a701219e](https://doi.org/10.1039/a701219e)
- p) J.Ribas, M.Monfort, B.K.Gosh, X.Solans, M.Font-Bardia, *Chem.Commun.* (1995), 2375, doi: [10.1039/C399500023759](https://doi.org/10.1039/C399500023759)
- q) M.Monfort, I.Resino, J.Ribas, X.Solans, M.Font-Bardia, P.Rabu, M.Drillon, *Inorg.Chem.* (2000), **39**, 2572, doi:[10.1021/ic991366j](https://doi.org/10.1021/ic991366j)
- r) Zhon Shen, Jing-Lin Zuo, Zhi Yu, Yong Zhang, Jun-Feng Bai, Chi-Ming Che, Hoong-Kun Fun, J.J.Vittal, Xiao-Zeng You, *J.Chem.Soc., Dalton Trans.* (1999), 3393, doi:[10.1039/a903968f](https://doi.org/10.1039/a903968f)